

iPSC-based restoration of ovarian function following gonadotoxic chemotherapy

iPSC-Derived Ovarian Tissue Restores Ovarian Function in Subfertile Mice After Gonadotoxic Chemotherapy

Elias, K.M.¹, Ng, N.W.², Dam, K.U.², Milne, A.², Disler, E.R.², Gockley, A.¹, Dunn, N.¹, Ginsburg, E.S.², and Anchan, R.M.^{2*}

¹Division of Gynecologic Oncology, Department of Obstetrics, Gynecology and Reproductive Biology, Brigham and Women's Hospital, Division of Gynecologic Oncology, Dana-Farber Cancer Institute, Harvard Medical School, Boston, MA 02115.

²Division of Reproductive Endocrinology and Infertility, Center for Infertility and Reproductive Surgery, Department of Obstetrics, Gynecology and Reproductive Biology, Brigham and Women's Hospital, Harvard Medical School, Boston, MA 02115.

Corresponding Author:

Raymond M. Anchan, MD, PhD

²Division of Reproductive Endocrinology and Infertility,
Department of Obstetrics, Gynecology and Reproductive Biology,
Brigham and Women's Hospital, Harvard Medical School, Boston, MA 02115.

Running Title: iPSC-based restoration of ovarian function following gonadotoxic chemotherapy

Abstract

Many oncologic therapies given to young women are gonadotoxic and associated with diminished ovarian reserve, increased risk of permanent sterility, and premature menopause. Previously, we reported the derivation of steroidogenic ovarian cells from induced pluripotent and embryonic stem cells. Derived cells not only produced reproductive hormones, but also displayed markers of ovarian tissue and primordial gametes. Here, we describe that human follicular fluid, when added to our stem cell differentiation system, enhances the steroidogenic potential of derived cells and increases the subpopulation of cells that differentiate to express the ovarian and germ cell markers GJA1 and ZP1, respectively. More importantly, using an *in vivo* model of chemotherapy-induced premature ovarian insufficiency in subfertile nude mice, we demonstrate that orthotopic implantation of these derived cells restores ovarian hormonal production and produces functional stem cell-derived germ cells. Collectively, these data support the hypothesis that stem cell-derived steroidogenic ovarian tissue could be used to promote neo-gametogenesis and treat premature menopause.

Introduction

Despite significant and rapid advances in assisted reproductive technologies (ART), few fertility-preserving options remain for women of reproductive age who have cancer and are planning chemotherapy¹. Many chemotherapeutic regimens are gonadotoxic, leaving women with compromised fertility after treatment. Currently, the most reliable method for fertility preservation is pre-chemotherapy fertility treatment cycles using ART to induce the growth of multiple oocytes for cryopreservation, either as oocytes or after fertilization as embryos^{2,3}. Unfortunately, referral rates for ART prior to commencing gonadotoxic chemotherapy are low⁴. Moreover, compared to similar women without cancer, even women with apparently preserved ovarian function after chemotherapy are more likely to experience infertility as well as less success from ART cycles with autologous oocytes^{5,6}. This is compounded in this patient population by the fact that some mutations which predispose women to cancer, such as *BRCA1* and Fanconi Anemia pathway members, are also associated with premature ovarian insufficiency^{7,8}.

Beyond infertility, premature ovarian insufficiency following chemotherapy treatment causes additional sequelae of estrogen deficiency⁹. Cancer survivors experience accelerated bone loss, increased sexual dysfunction, and higher rates of cardiovascular mortality compared to their age-matched peers without cancer^{10–13}. Restoration of hormones is primarily accomplished by exogenous hormone replacement therapy (HRT); however, there is limited data on the long-term health consequences of prolonged HRT in adolescents and young women, raising concerns about increasing risks of secondary malignancies^{14–16}. This has led to calls to develop new technologies to preserve or restore ovarian function¹⁷.

In this study, we present a novel and exciting approach to the treatment of infertility by generating functional oocytes derived from induced pluripotent stem cells. We previously reported that embryonic stem cells (ESCs) and induced pluripotent stem cells (iPSCs) may be differentiated into steroidogenic ovarian cells that produce physiologic concentrations of the reproductive hormones estrogen and progesterone^{18–20}. iPSCs generated from mouse granulosa cells (mouse granulosa cell-derived iPSCs, or mGriPSCs) preferentially differentiate into homotypic ovarian cell types due to their epigenetic memory¹⁸. By using patient-specific iPSCs to generate steroidogenic ovarian tissue, these derived cells can be syngeneic with the patient. Here, we show that differentiation of mouse iPSCs into steroidogenic reproductive ovarian tissue *in vitro* is enhanced by media containing human follicular fluid. Following differentiation, we demonstrate that these ovarian and primordial oocytes can be isolated through fluorescence-activated cell sorting (FACS) using a cell surface receptor for a biochemical marker of ovarian reserve, anti-Mullerian hormone receptor 2 (AMHR2). While the FACS-sorted heterogenic population of stem cells is enriched for AMHR2 immunoreactivity, the associated stem cell derived precursors still retain the capacity to differentiate into granulosa like steroidogenic cells as well as gametes. Most importantly, injection of the stem cell-derived AMHR2+ enriched cell population into subfertile mice exposed to gonadotoxic chemotherapy restores ovarian function as indicated by both the recovery of steroidogenic production and *de novo* generation of stem-cell derived gametes. Finally, we show that these stem cells can trigger activation of the endogenous oogenesis process to produce functionally mature oocytes as demonstrated by their capacity for fertilization and activation via a calcium ionophore towards the generation of parthenotes²¹.

Results

Differentiated iPSCs regenerate steroidogenic reproductive ovarian tissue *in vitro*.

Age-matched normal mouse ovarian tissue (Fig. 1 I. A-C) and *in vitro* differentiated mGriPSCs at 2 weeks post-attachment (Fig. 1 II. A-C) expressed comparable antigen profiles (Fig. 1 I. D-O and II. D-L) for the ovarian and germ cell markers AMHR2, CYP19A1, FOXL2, FSHR, INHB, DAZL, DDX4, ZP1, and ZP2 using immunofluorescent staining. Expression of these markers in the differentiated mGriPSCs was also confirmed by RT-PCR (Fig. 1 III). Steroidogenic activity in embryoid bodies (EBs) from the differentiated mGriPSCs was confirmed by ELISA, which detected physiological concentrations of estradiol in culture media during extended cell culture (Fig. 1 IV).

Human follicular fluid promotes efficient differentiation of iPSCs into steroidogenic ovarian tissue and enhances expression of ZP1 and GJA1.

mGriPSCs were cultured with media containing 1% or 5% human follicular fluid (HFF) obtained at the time of oocyte retrieval. HFF, collected as pooled samples from multiple patients, was found to contain estradiol (mean > 3,000 pg/mL), FSH (mean = 14.20 IU/L, range = 16.85 IU/L), and LH (mean = 0.26 IU/L, range = 0.27 IU/L). The addition of HFF markedly increased the estradiol synthesis by mGriPSCs over 15 days in culture (Fig. 1 V). Additionally, HFF promoted increased expansion of a subpopulation of cells expressing the granulosa cell marker GJA1²² and the oocyte marker ZP1 (Fig. 1 VI).

iPSC -based restoration of ovarian function following gonadotoxic chemotherapy

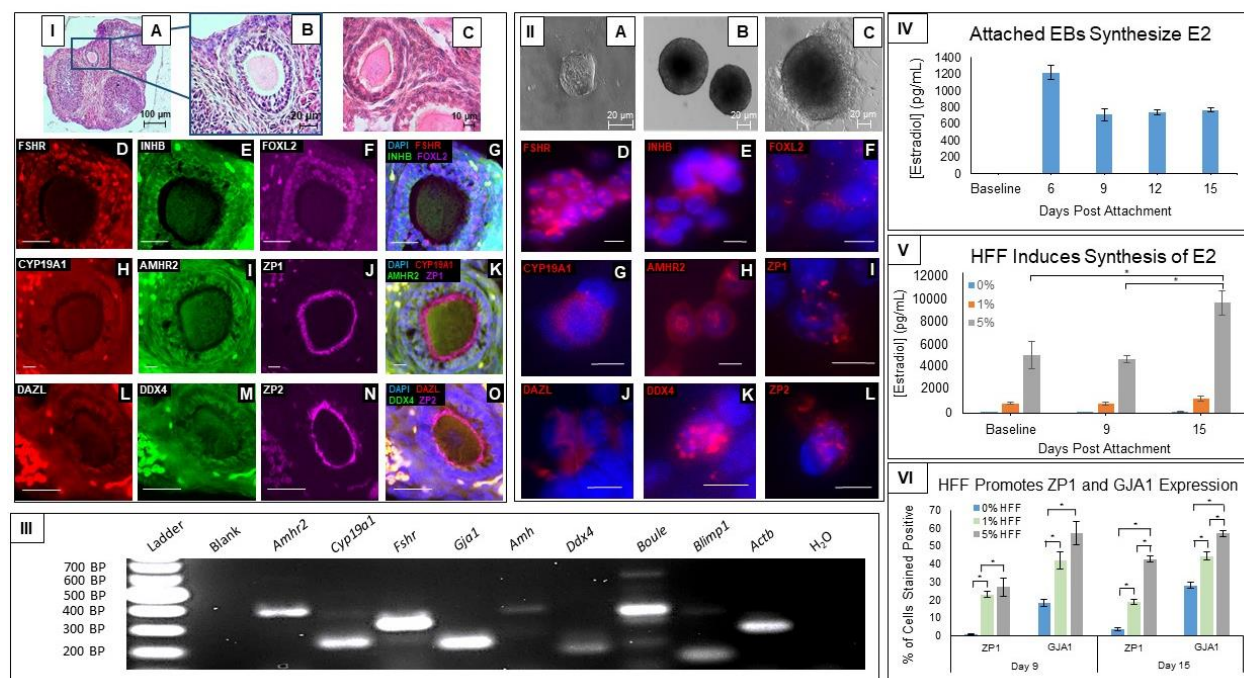


Figure 1. mGriPSCs differentiate into steroidogenic cells that express ovarian and oocyte markers. *In situ* hematoxylin & eosin (H&E) staining of mouse ovarian sections shows follicles (I. A-C). Immunohistochemistry (IHC) of mouse follicles demonstrates localization of the known ovarian antigens FSHR, INHB, FOXL2, CYP19A1, AMHR2 (I. D-I) and oocyte markers ZP1, ZP2, DAZL, DDX4 (I. J-O). *In vitro* phase-contrast images of a mGriPSC colony (II. A), mGriPSC embryoid bodies (EBs) at two weeks post-suspension (II. B), and an attached mGriPSC EB (II. C). Immunocytochemistry (ICC) shows that differentiated mGriPSC EBs at 15 days post-attachment also express the same corresponding ovarian (II. D-H) and oocyte antigens (II. I-L). Transcriptome analysis using RT-PCR confirms synthesis of these as well as other related ovarian tissue transcripts in these mGriPSCs EBs (*Amhr2*, *Cyp19a1*, *Fshr*, *Gja1*, *Amh*, *Ddx4*, *Boule*, *Blimp1*; III). ELISA reveals that differentiated EBs also synthesize the reproductive ovarian hormone, estradiol (E2), at physiologically relevant levels (710-1220 pg/mL) over 15 days (IV; n=3). The addition of 5% human follicular fluid (HFF) to culture media enhances E2 synthesis in mGriPSCs (V; n=3, Mann-Whitney U test, $P < 0.05$). 1% and 5% HFF in media also promotes increased expression of an oocyte marker ZP1 (zona pellucida 1) and a granulosa cell marker GJA1²¹ (gap junction protein alpha) according to ICC positive cell counts (VI; n=7, Mann-Whitney U test, $p < 0.003$). Scale bars in I. D-O, 25 μ m; in II. D-L, 10 μ m. Data represented as mean \pm SEM.

Stem cell-derived ovarian tissue retains endocrine function and expression of ovarian markers when purified via fluorescence-activated cell sorting (FACS).

After derivation *in vitro*, mGriPSCs were stably transfected with a green fluorescent protein (GFP) reporter using a lentivirus, followed by differentiation into ovarian tissue as previously described^{18,20} (Fig. 2A). RT-PCR confirmed that mGriPSCs-GFP retain expression of pluripotency markers (Supp Fig. 1A). These cells were then sorted by FACS using a cell surface level antigen, AMHR2, specific to differentiated ovarian tissue (Fig. 2B) and confirmed by RT-PCR to be expressed in mouse oocytes (Supp Fig. 1B). ELISA revealed preservation of estradiol and progesterone synthesis capacity in both pre- and post-sorted cells (Fig. 2C-E). ICC indicated retained expression of ovarian antigens AMHR2, CYP19A1, and GJA1 in pre-sorted (Fig. 2F-H)

iPSC -based restoration of ovarian function following gonadotoxic chemotherapy

and post-sorted cells (Fig. 2I-K). RT-PCR further confirmed these results, as indicated by the retention of RNA transcript expression of ovarian and oocyte-specific genes (*Amhr2*, *Cyp19a1*, *Fshr*, *Gja1*, *Amh*, *Ddx4*, *Boule*, and *Blimp1*; Fig. 2L, M). Sorting mGriPSCs with AMHR2 thus led to a heterogeneous population of differentiated cells that comprised of both putative granulosa cells and oocytes.

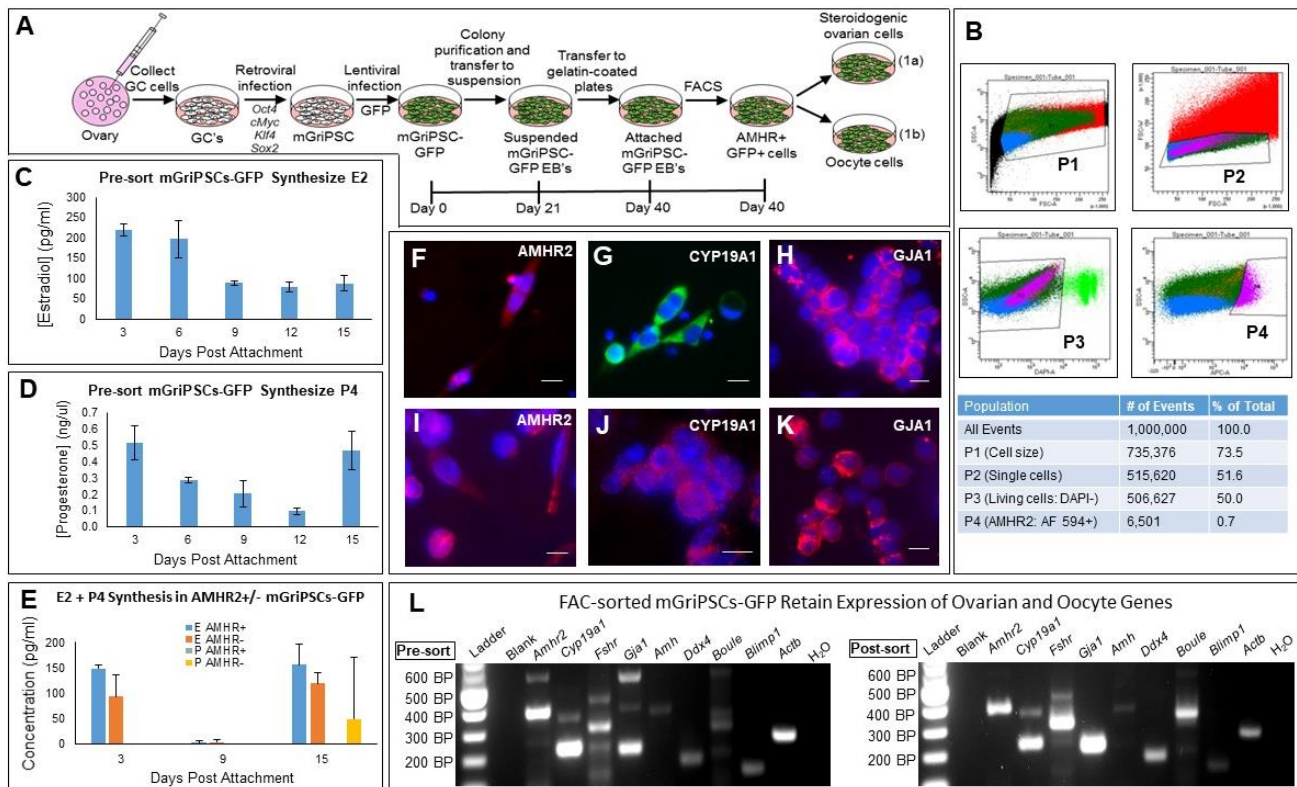


Figure 2. Fluorescence activated cell sorting (FACS) purifies functional iPSC-derived steroidogenic ovarian cells. Schematic representation of the experimental flow for generation of mGriPSCs, green fluorescent protein (GFP) labeling, differentiation, and FACS purification of AMHR2+ mGriPSCs-GFP (A). FACS reveals 0.7% of the total population of mGriPSCs-GFP positively expresses ovarian antigen AMHR2 (P4 population; B). Pre- and post-sorted mGriPSCs-GFP synthesize E2 and progesterone (P4) through 15 days in culture (C, D), while post-sorted cells primarily produce E2, consistent with our prior observations¹⁷ (E). ICC shows that differentiated mGriPSCs-GFP both before (F-H) and after (I-K) FACS express the ovarian antigens AMHR2, CYP19A1, and GJA1. The expression of these ovarian markers is further supported by RT-PCR transcriptome analysis of pre- and post-sorted cells (*Amhr2*, *Cyp19a1*, *Fshr*, *Gja1*, *Amh*, *Ddx4*, *Boule*, and *Blimp1*; L). Scale bars in F-K, 10 μ m. n=3, data represented as mean \pm SEM.

Alkylating chemotherapy leads to accelerated follicular atresia and breast atrophy in nude mice.

In humans, gonadotoxicity of chemotherapeutic agents is highly variable and dependent on dose, patient age, and prior ovarian reserve. Dosing related toxicity is influenced by absolute and cumulative dosing. Nearly 30% of breast cancer cases present in women younger than 50 years old. While newer treatment regimens employed are less gonadotoxic, regimens still consist of combination medications that include cyclophosphamide, known to deplete the number of primordial follicles, thereby potentially leading to infertility. For common regimens such as Adriamycin/Cytosan (AC), the risk of premature ovarian failure is thought to be largely dependent on patient age, with the risk of complete ovarian failure at less than 10% in women under 30, and nearly 100% in women over 40²³; however, other studies indicate that AC is considered to have intermediate risk for gonadotoxicity in women over 40.

Nude mice are known to be subfertile due to age-related rapid follicular atresia²⁴. To model the additive impact of alkylating chemotherapy to a subfertile population, nude mice received single intraperitoneal injections of busulfan (12 mg/kg) and cyclophosphamide (120 mg/kg) or 100 μ l of vehicle (10% DMSO in PBS; Fig. 3A). Within 63 days of chemotherapy injections, mice exhibited a complete loss of estradiol production (Supp Fig. 2B), in addition to breast atrophy (Supp Fig. 2A). At necropsy, mice that received gonadotoxic chemotherapy displayed smaller ovaries with fewer follicles (Fig. 3C) compared to age-matched controls (Fig. 3D). This accords with previous mouse studies in which the gonadotoxic effects of cyclophosphamide and busulfan have been demonstrated²⁵.

The mouse studies demonstrated a global loss of ovarian follicles, marginal atrophy, and a presumably increased risk for ovarian failure and infertility after the chemotherapeutic gonadotoxic insult. Therefore, this mouse model resembles the clinical paradigm encountered by reproductive age women undergoing chemotherapy by showing a chemically-mediated decrease in follicle size and number as opposed to a complete elimination.

FACS-sorted AMHR2+ mGriPSCs restore hormonal function but do not form teratomas.

We have previously shown that mGriPSCs produce estradiol, but like all iPSCs, these form teratomas when injected into mice²⁶ (Fig. 3E; Supp Fig. 2C). We hypothesized that sorting mGriPSCs based on the expression of cell surface protein AMHR2 might allow selection of a more differentiated cell type, thereby minimizing the risk of tumor formation. Six-week old nude female mice underwent estrous synchronization with PMSG, followed 48 hours later by human chorionic gonadotropin (hCG). Three weeks later, experimental mice received single intraperitoneal injections of busulfan (12 mg/kg) and cyclophosphamide (120 mg/kg), while control mice received 100 μ l of vehicle (10% DMSO in PBS). After three additional weeks, experimental mice received intramuscular injections into the left thigh of either vehicle, FACS-purified AMHR2+ mGriPSCs or unsorted mGriPSCs. Before the stem cell injections, breast atrophy in the chemotherapy exposed mice had been noticeable (Fig. 3B), indicative of estrogen deficiency. Within 72 hours of stem cell injection, the breast atrophy had been reversed in the mice receiving sorted or unsorted cells (Fig. 3B), suggesting restoration of estradiol production. Mice were followed for an additional one month. While all mice receiving unsorted cells developed large teratomas, no macroscopic or microscopic teratomas were seen in mice receiving sorted cells (Fig. 3E,F).

iPSC -based restoration of ovarian function following gonadotoxic chemotherapy

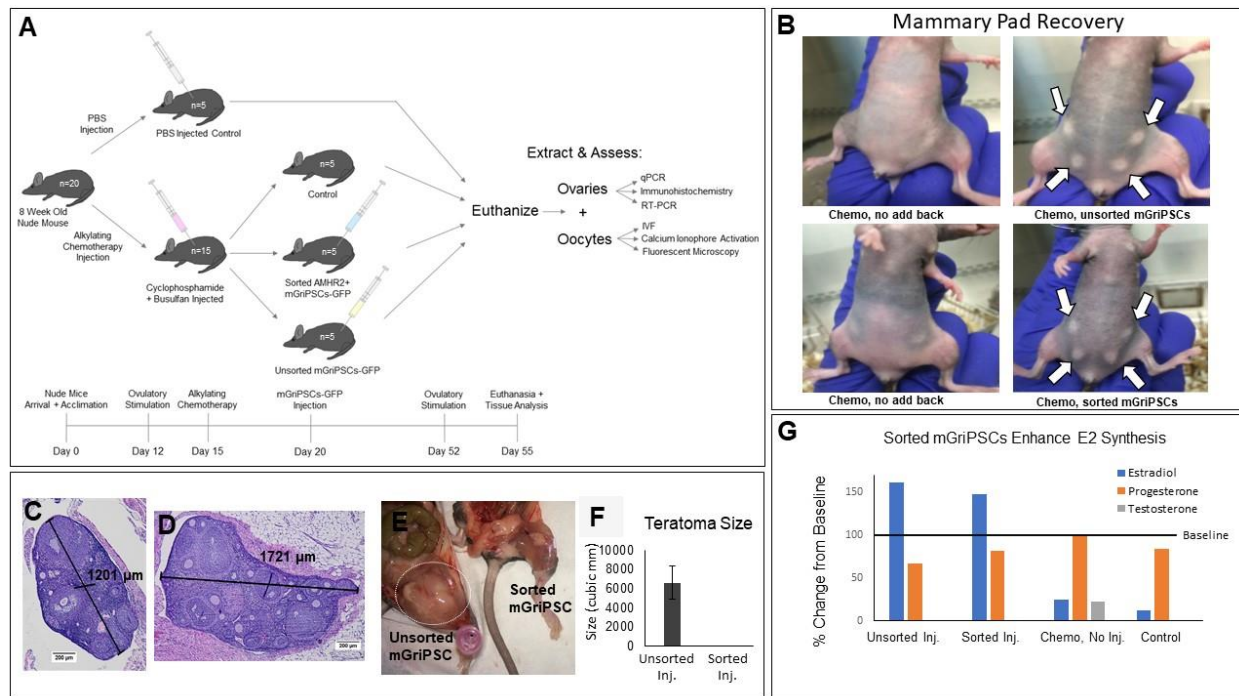


Figure 3. AMHR2+ sorted mGriPSCs-GFP preserve estrogen effects but do not form teratomas.

Schematic representation of *in vivo* experimental flow for ovarian injections (A). Following alkylating chemotherapy, mice injected intramuscularly with sorted or unsorted mGriPSCs show evidence of mammary pad restoration after 72 hours, whereas mice that did not receive mGriPSCs show no mammary pad recovery (B). H&E staining revealed partial ovarian atrophy after chemotherapy exposure, as indicated by a decrease in ovary size and fewer follicles (C) compared to a control ovary (D). Injecting FACS-purified cells prevents the formation of teratomas, as compared with unsorted cell injections (data represented as mean \pm SEM; E,F). Compared to mice that receive chemotherapy without mGriPSCs injections, mice that receive sorted or unsorted mGriPSCs injections after chemotherapy show an increase in blood E2 levels (G; n=3, data represented as mean percent change in hormone concentrations before and after mGriPSCs injections, as measured by ELISA). As previously reported, since E2 is the predominant reproductive hormone synthesized by differentiating mGriPSCs, P4 is observed to remain unchanged under all conditions¹⁷ (G). Testosterone is only detectable in mice that receive chemotherapy but no mGriPSCs injections (G).

Orthotopic intraovarian injections of stem cell-derived ovarian tissue produces *de novo* generation of functional granulosa cells and mature oocytes *in vivo*.

While intramuscular injections of AMHR2+ mGriPSCs appeared to preserve hormonal function in chemotherapy treated mice, because of the absence of tumor formation, we were not technically able to retrieve the cells for subsequent analysis. Therefore, we next investigated the effect of orthotopic injection of mGriPSCs-GFP. Mice underwent estrous synchronization and then received alkylating chemotherapy. Rather than allowing the follicles to atrophy completely as in

the prior experiments, we planned a shorter time interval for stem cell injections to model a rescue therapy. Therefore, the following week, mice received direct intraovarian injections of GFP-labelled unsorted or sorted AMHR2+ mGriPSCs via laparotomy. Shortening the timeframe between chemotherapy and stem cell administration also made it easier to perform surgical manipulation of the ovaries before they became too atrophic. Mice were then followed for one month. Mice then underwent a second 48-hour cycle of PMSG/hCG ovarian stimulation, followed by euthanasia.

Oocytes were then collected directly from the ovaries by puncturing the bursa *ex vivo* and flushing the oviducts. Mature oocytes collected from mice injected with sorted mGriPSCs-GFP not only expressed GFP under fluorescent microscopy (Fig. 4A,B; Supp Fig. 3A-M), but also displayed evidence of both calcium ionophore activation (Fig. 4C; Supp Fig. 3J-M) and fertilization (Fig. 4D; Supp Fig. 3D-I). RT-PCR analysis on these oocytes showed co-expression of *Sry* and *Gfp*, confirming successful fertilization and mGriPSCs-GFP lineage (Fig. 4H). Further, the *in-situ* (Fig. 4E) and *ex vivo* (Fig. 4F) expression of GFP in granulosa cells of mGriPSCs-GFP treated mice supports the *de novo* generation of stem cell-derived ovarian tissue, in addition to oocytes. Ovarian follicle immunosections from mice injected with sorted cells also expressed GFP, which co-localized with AMHR2 and DAZL (Supp Fig. 3N,O). Additionally, quantitative reverse transcription PCR (RT-qPCR) indicated increased *in vivo* expression of terminal oocyte marker *Zp1* in the ovaries that received the sorted mGriPSCs-GFP injection compared to the contralateral uninjected ovaries and the ovaries of mice that received chemotherapy but no stem cell injections (Supp Fig. 4). After gonadotropin hyperstimulation, 18 mature oocytes were recovered from the mouse ovaries that were previously orthotopically injected with sorted cells, whereas five oocytes were collected from these mice's contralateral ovaries in which no cells were injected. Of these 18 retrieved oocytes, eight expressed GFP (Fig. 4G; Supp Fig. 3), indicative of their stem cell origin. This suggests neogametogenesis, as well as salvation of native oocytes through paracrine effects. No oocytes were collected from the left ovaries of the mice injected with unsorted cells, as large teratomas obstructed the collection process (Supp Fig. 2C).

Injection of unsorted differentiated mGriPSCs-GFP into the ovary yielded the highest increase in estradiol production from pre- to post-stem cell injection conditions (Fig. 3G), consistent with prior observations in which heterotypic differentiated EBs synthesized high levels of steroid hormones^{18–20,27}. Further, in alignment with our prior studies, the progesterone synthesis between different experimental groups was not significantly different (Fig. 3G), as mGriPSCs appear to preferentially differentiate into estradiol synthesizing granulosa cells, presumably the consequence of their epigenetic memory. ELISA detected testosterone production in only the group that received alkylating agents without stem cell injections (Fig. 3G). Testosterone measurements support the hypothesis that observed differences between groups in estradiol levels, which is synthesized from testosterone via aromatase, are not restricted by availability of substrate. Together, this shows that AMHR2+ mGriPSCs-GFP can produce both functional granulosa cells and mature oocytes.

iPSC -based restoration of ovarian function following gonadotoxic chemotherapy

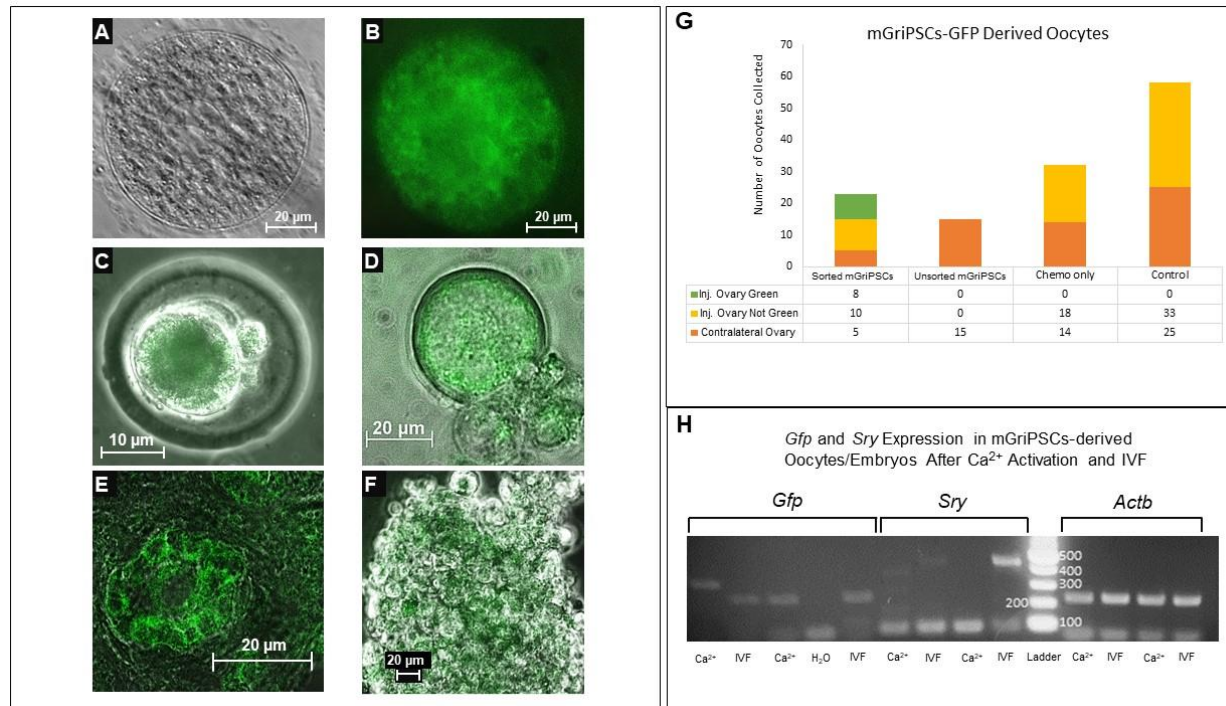


Figure 4. Neogametogenesis with differentiated iPSCs *in vivo*. Images A-F depict cells and tissues collected from mouse ovaries exposed to gonadotoxic chemotherapy followed by injection of sorted mGriPSCs-GFP. Corresponding phase contrast (A) and fluorescent microscopy (B) images of a mature oocyte expressing GFP. Maturation and functionality of GFP-labeled oocytes is supported by the ability to activate with calcium ionophore (A23817; C) and fertilize *in vitro* (D). IHC indicates localization of GFP to granulosa cells of the follicle (E). Isolated granulosa cells also express GFP (F). Oocytes with and without GFP expression are counted in mice from all treatment groups, in both the ovary injected with stem cells and the contralateral ovary (G). RT-PCR transcriptome analysis confirms *Gfp* expression in these calcium ionophore activated oocytes and IVF embryos, as well as *Sry* expression in IVF embryos (H). Collectively, these results demonstrate that orthotopic injection of sorted, GFP-labeled mGriPSCs following chemotherapy contributes to follicular formation and *de novo* generation of oocytes.

Anti-Mullerian hormone synthesis is observed in stem cell treated mice.

AMH is typically observed in the native ovary and is a marker for ovarian follicular reserve. The differentiated mGriPSCs-GFP that were sorted and later injected into mouse ovaries demonstrated AMH synthesis *in vitro* (Supp Fig. 6O) as well as in the tissue (Fig. 5A,B) and serum (Fig. 5C) from mice treated with mGriPSCs-GFP. As expected, chemotherapy accelerated the reduction in AMH levels compared to control mice (Fig. 5C). In contrast, AMHR2+ mGriPSCs preserved AMH levels *in vivo*, an effect not seen with unsorted mGriPSCs (Fig. 5C). Interestingly, when we compared *Amh* mRNA levels between the left ovary, which received AMHR2+ mGriPSCs-GFP, and the right ovary, which did not, *Amh* expression was high in both ovaries compared to chemotherapy exposed ovaries from mice that did not receive mGriPSCs (Fig. 5D).

Stem cell-derived ovarian tissue supports oogenesis in co-culture.

An exciting novel finding in our study is the terminal functional differentiation of *de novo* generated gametes from iPSCs (Fig. 4). We hypothesized that this is, in part, a consequence of recreating the ovarian microenvironment that supports oocyte development. Undifferentiated mGriPSCs, suspended EBs, or attached EBs were grown in transwells overlying a feeder layer of FACS-

purified AMHR2+ mGriPSCs-GFP (Supp Fig. 5). This AMHR2+ cell population reproduced the function of ovarian tissue, as confirmed by transcriptome RT-PCR analysis (Supp Fig. 6L). Under these co-culture conditions, we observed the differentiation of mGriPSCs into gametes that expressed oocyte marker DDX4, as well as the terminal oocyte marker ZP1 (Supp Fig. 6A-I). Furthermore, such differentiated cells were sorted to reveal positive expression of oocyte antigens using FACS (Supp Fig. 6J,K). FACS showed that compared with suspended EBs co-cultured with other feeder layers (1. No cells, 2. Irradiated mouse embryonic fibroblasts, 3. Mouse G4 ESCs, or 4. Unsorted mGriPSCs-GFP), suspended EBs co-cultured with AMHR2+ mGriPSCs-GFP exhibited greater expression of late female oocyte markers ZP2 and BOULE (Supp Fig. 6J,K and Supp Fig. 7,8). Further, RT-qPCR demonstrated that suspended EBs co-cultured with sorted mGriPSCs-GFP expressed increased levels of oocyte markers ZP1 and DDX4 compared to EBs that were co-cultured with unsorted mGriPSCs-GFP (Supp Fig. 6M). We also observed a retention of estradiol synthesis for all co-culture conditions (Supp Fig. 6N).

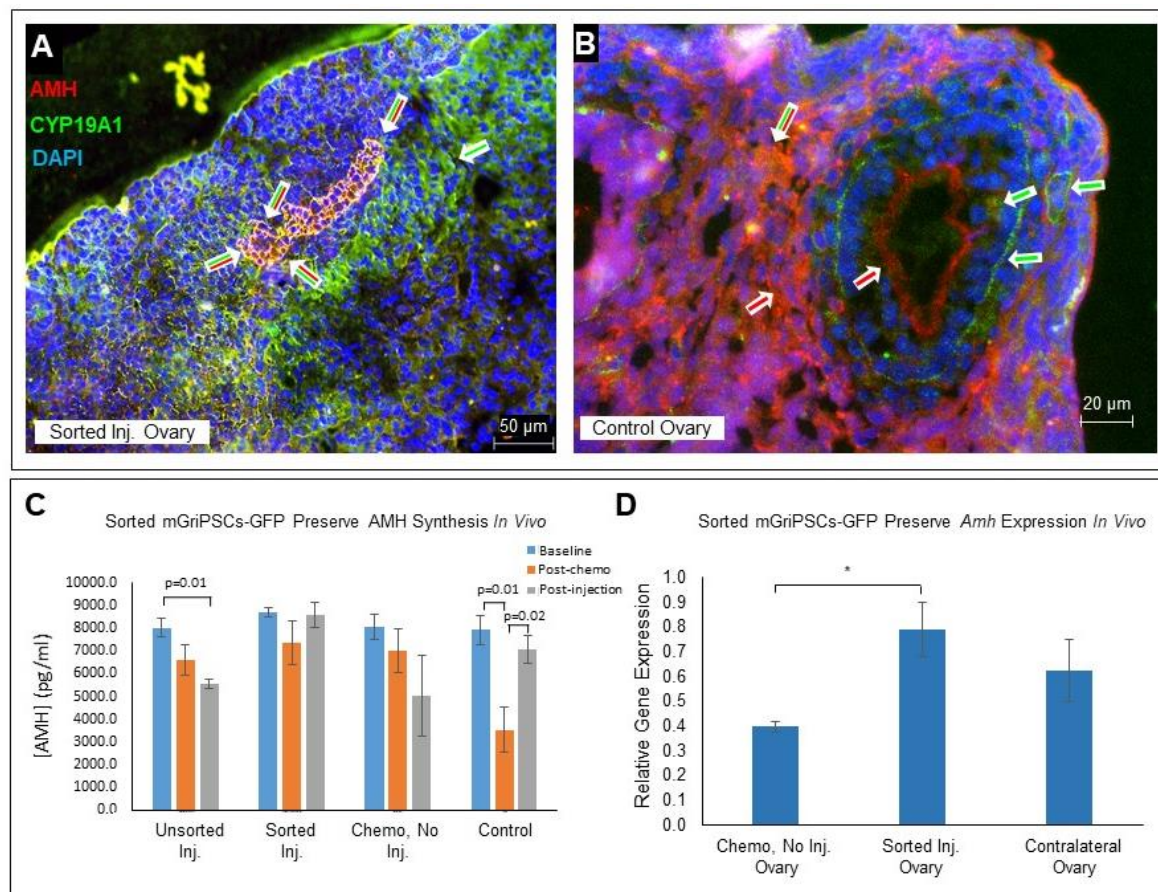


Figure 5. Sorted mGriPSCs-GFP synthesize AMH *in vivo*. IHC of an ovary injected with sorted mGriPSCs-GFP confirms estradiol and AMH synthesis (A), as compared with a control ovary (B). Mice exposed to chemotherapy show reduced AMH synthesis, but those that receive sorted mGriPSCs-GFP injections retain AMH synthesis after stem cell injections (C; $n=3$, Mann-Whitney U; data represented as mean \pm SEM, as measured by ELISA). RT-qPCR analysis on RNA extracted from ovaries exposed to chemotherapy reveals greater expression of *Amh* in mice injected with sorted cells compared with those that were not injected with stem cells (D; $n=3$, Mann-Whitney U, $p<0.05$; data represented as mean gene expression fold change \pm SEM, as compared with control ovary gene expression).

Discussion

In this study, we report a potential autologous iPSC system for the *de novo* generation of functional oocytes. While early studies have shown differentiation of murine embryonic stem cells to express primordial germ cell markers²⁸, the capacity to mature these cells *in vitro* and to fertilize them has been difficult. Recent observations suggest that the ovarian cortex plays a central role in mediating the maturation and development of primordial germ cells^{29,30}. The ovarian cortex is comprised of stroma and functional follicles. The primary follicular cell types include mural and cumulus granulosa cells that line the antrum of the follicle, which also contains the primordial oocyte. The primary endocrine cells of the ovary are the thecal cells, which make androgens, and the granulosa cells, which produce estrogen and progesterone from the androgen precursors.

The current study builds upon our prior report demonstrating the homotypic differentiation of murine granulosa cell-derived iPSCs into steroidogenic ovarian tissue^{18,20}. In the current work, we show that this stem cell-derived ovarian cortex also supports increased generation of differentiating stem cells that express oocyte markers, presumably a larger cohort of primitive oogonia. While the feasibility of generating stem cell derived oocytes using reconstituted ovarian tissue has been described¹⁸, our work for the first time shows that oocyte development and the supporting ovarian cortical matrix can both be promoted directly from induced pluripotent stem cells^{31,32}. A key observation in these studies is the capacity for differentiated, sorted mGriPSCs to contribute to the *de novo* generation of oocytes, as well as form ovarian follicles as evidenced by the GFP labelled follicular granulosa cells. What remains unclear after FACS purification is whether: 1) Two distinct types of AMHR2+ precursors arise that lead to oocyte or granulosa cell lineages, or 2) A common, AMHR2+ stem cell-derived precursor arises that later differentiates into either oocytes or granulosa cells. Of note, RT-PCR analysis of native mouse oocytes revealed co-expression of AMHR and ZP1. Therefore, the generation of two cell types from AMHR+ sorted cells seems highly plausible and supports the notion that mGriPSCs are regenerating ovarian tissue.

We found that oocyte generation from mGriPSCs was enhanced by using human follicular fluid, analogous to what one observes *in vivo*, wherein primordial germ cells are bathed in follicular fluid during critical portions of their development. HFF used in these experiments contained FSH (6-23 IU/L), LH (0.1-0.37 IU/L) and estradiol (>3000 pg/mL). The resulting differentiated stem cells generated autologous steroid hormones and expressed normal markers of germ cells and granulosa cells. The phenotypic evidence of endocrine recovery in chemotherapy treated mice (i.e. restoration of the mammary pads) was notable as early as 72 hours after injection of the differentiated stem cells. We also observed that gonadotropin-induced ovarian hyperstimulation resulted in an appropriate physiologic response with maturation of follicles and gametes, further supporting the conclusion that the stem-cell derived ovarian endocrine cells exhibit normal endocrine behavior comparable to native ovarian cortex.

Finally, we show that the orthotopic injection of these differentiated, FACS-sorted stem cells into nude mice following chemotherapy facilitates resumption of oocyte development and the *de novo* generation of stem cell-derived oocytes. This is demonstrated by the presence of GFP-oocytes in these nude mice. More importantly, the ability to fertilize and use a calcium ionophore to activate these stem cell-derived oocytes demonstrates functional neo-gametogenesis. Interestingly, injection of these AMHR2+ mGriPSCs-GFP into a single ovary of nude mice following chemotherapy also improved endocrine function in the contralateral ovary. The capacity to rescue the contralateral ovary suggests this is mediated by a paracrine mechanism. This agrees with

observations from other groups describing the potential role for paracrine mechanisms mediated by injected bone marrow and mesenchymal stem cells for chemoprotection of ovaries^{33–35}.

The precise paracrine mechanism of action remains elusive for those stem cells, however, AMH proves to be a promising candidate molecule given its preventative effect on follicular atresia and apoptosis^{36,37}. AMH is exclusively synthesized by granulosa cells during the early stages of follicular development³⁸, and AMH serum concentration is an important measure of ovarian reserve³⁹. Additionally, the effect of gonadotoxic agents on ovarian follicular development is reflected by lower serum concentrations of AMH^{40,41}. Moreover, low AMH levels are prognostic for poor probability of spontaneous conception as well as poor response to ART⁴². Post-chemotherapy AMH levels are also an important biomarker for early onset of menopause⁴³.

As such, we explored AMH synthesis in our experimental animals that received stem cell injections, observing a concurrent increase in AMH synthesis. The observation of restored contralateral ovarian function along with the finding of elevated AMH synthesis by the differentiated stem cells, collectively supports the idea that AMH may be important in mediating the observed restoration of ovarian function in these studies^{33–37}. Together, these data suggest the feasibility of patients providing their own cells to restore ovarian function, synthesize bioidentical hormones, and restore fertility by neogametogenesis.

The endogenous resumption of oocyte development in stem cell treated mice is remarkable given the marked atrophy of ovarian tissue in the treated mice without injection of stem cells. Additionally, the capacity to generate physiologic concentrations of estradiol and progesterone offers patients the option of using endogenous hormones for replacement therapy. By applying this to microfluidic chip technology, patient specific steroidogenic cells can be cultured within a sterile, continuously flowing environment (Fig. 6). Personalized reproductive hormones (progesterone, estradiol, testosterone, and AMH) can be generated and utilized by specific extraction from conditioned media. These personalized hormones could be used for hormone replacement therapy (HRT) as well as *in vitro* egg maturation. We believe that these findings collectively afford us the unique opportunity to develop novel therapeutic options for cell-based therapies, especially relevant for women with premature ovarian failure (Fig. 6).

iPSC -based restoration of ovarian function following gonadotoxic chemotherapy

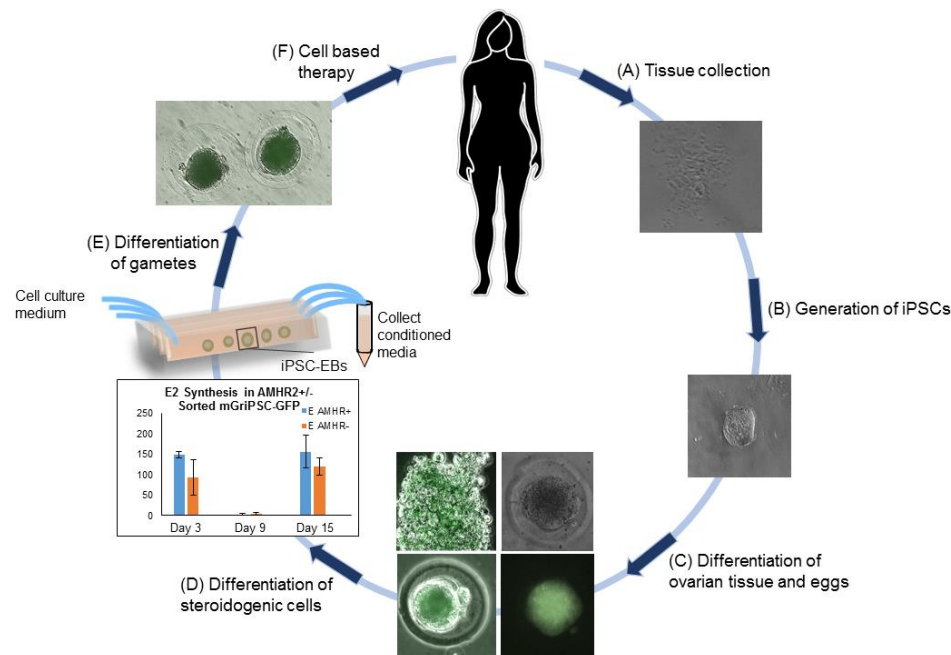


Figure 6. An autologous stem cell-based model for fertility and endocrine function restoration.

A model for translational applications of this research. Somatic cells are collected from a patient (A) and converted into autologous iPSCs (B). These iPSCs are differentiated into ovarian steroidogenic and reproductive cells (C, D). Microfluidic chip technology may be utilized to create a sterile, continuously flowing environment, creating the ability to purify autologous bioidentical reproductive hormones from the conditioned media (D). The autologous oocytes (E) and endogenous steroid hormones (D) may then be collected and used to treat the same patients, ultimately restoring fertility and endocrine function (F).

We do acknowledge several limitations to our study. First is the use of granulosa cell-derived iPSCs. To determine whether our endocrine differentiation observations may be extended to other iPSC types, we have previously investigated fibroblast and amniocyte derived iPSCs as well as embryonic stem cells with similar results, although with a lower efficiency^{18,20}. We believe the higher efficiency of mGriPSCs in generation of ovarian endocrine tissue relates to the epigenetic memory of these cells. However, the observed ability to differentiate other iPSC types along this pathway potentially benefits a larger number of patients who may not have had the opportunity to attempt IVF and harvest granulosa cells prior to their chemotherapy or who have had oophorectomies and no longer have ovarian tissue present. Second, while we have shown that AMHR2+ mGriPSCs can rescue ovaries exposed to chemotherapy, we have not tested whether AMHR2+ mGriPSCs can be derived from ovaries that have already received a gonadotoxic insult. We have also not tested the ability to impact other gonadotoxic insults, such as radiation therapy. Additionally, we have not evaluated the normalcy of these stem cell derived oocytes. Finally, while we have shown embryos derived from GFP-positive AMHR2+ mGriPSCs, we did not transfer these embryos to a surrogate to investigate the viability of pups. We hope to address these limitations in future work.

In sum, the ability to generate patient specific bioidentical hormones, as well as autologous gametes, would revolutionize therapeutic options for women with chemotherapy related or idiopathic premature ovarian failure (up to 5% of the general population of women⁴⁴). In the future,

the successful generation of functional human gametes from iPSCs would be a major advancement in translational research.

Materials and Methods

All supplies were purchased from Sigma Aldrich (St. Louis, Missouri), unless otherwise stated. All antibodies were purchased from Abcam (Cambridge, MA; Supp Table S1) and all PCR primers were purchased from ThermoFisher (Waltham, MA). All protocols involving animals or using animal tissue have been approved by Brigham and Women's Hospital (BWH) Institution of Animal Care and Use Committee (IUCAC), detailed in protocol #2016N000367 or Dana Farber Cancer Institute (DFCI) Institution of Animal Care and Use Committee (IUCAC), detailed in protocol #15-047. All experiments were performed in accordance with relevant guidelines and regulations.

Cell lines

Mouse granulosa cells retrieval

Female C57BL6/J mice were purchased from Charles River Laboratories (Wilmington, MA) and followed by a veterinarian. In accordance with IUCAC approval, female C57BL6/J mice were hyperstimulated with pregnant mare's serum gonadotropin (PMSG) and human chorionic gonadotropin (HCG). The mice were subsequently sacrificed and their oocyte-GC-complexes collected and harvested using standard techniques. Hyaluronidase was then used to release the cumulus GCs surrounding each oocyte, and the resulting GCs were centrifuged at 1500 rpm.

Generation and expansion of mGriPSCs

Mouse granulosa cells were reprogrammed as previously described²⁶ to generate mouse granulosa-cell derived induced pluripotent cells (mGriPSCs). Briefly, employing standard retroviral production protocols using pMXs retroviral plasmids as vectors⁴⁵, mouse retroviral reprogramming vectors for iPSC genes, *Oct4*, *Sox2*, *c-Myc* and *Klf4*, were created. 293T cells, in DMEM and 10% HI FBS, were cultured until 40-50% confluency, and then transfected with the reprogramming vectors stated above, ecotropic envelope (ECO) and vesicular stomatitis virus-G glycoprotein (VSV-G) using FuGENE (Roche, Indianapolis, IN) for 48 hours before being harvested. Due to low proliferation rates in culture, the primary GCs were infected with the viral vectors and 8 µg/ml polybrene (Millipore, Burlington, MA) for 24 hours and then the viral media was rinsed. Cultures were observed for 2 weeks for the presence of stem cell-like colonies, which were manually picked by morphology and subcultured on mitomycin C-mitotically-inactivated mouse embryonic fibroblasts (MEFs; Global Stem, Rockville, MD) feeder layer. Stem cells were cultured in standard mouse stem cell media for several days. Mouse stem cell media contained DMEM, 10% ES-grade HI FBS, 1000 U/ml embryonic stem cell research oversight-leukemia inhibitory factor (ESCRO LIF; Millipore), 2 mM L-Glutamine (GIBCO), 0.2 mM 2-mercaptoethanol (BME). Stem cell colonies were picked based on morphology, passaged onto fresh MEF feeder plates, and further isolated by the identification of an external antigen characteristic of undifferentiated stem cells, stage-specific embryonic antigen-1 (SSEA-1; Millipore), through live-immunostaining. The positively stained stem cell colonies were then picked and further expanded.

GFP tagging through viral infection and stem cell pluripotency verification

Infecting mGriPSCs with green fluorescent protein (GFP) would allow the mGriPSCs and resulting differentiated cells to be labeled and tracked throughout our experimental process. The GFP gene was transfected into 293T cells by combining the GFP construct, VSV-G, and delta 8.2 lentiviral

packaging system with FuGENE and culture media. Using a fluorescent microscope (Nikon), the GFP signal was observed in transfected 293T cells. The viral containing culture media was harvested and mixed with 8 µg/ml polybrene to be fed onto healthy stem cell colonies. Resulting mGriPSCs expressing GFP were purified by dissociation and isolated by FACS machines. The GFP containing mGriPSCs from FACS were further purified with the described live-staining method and stem cell colonies were verified by PCR and immunocytochemistry (ICC) as well as an alkaline-phosphatase reaction kit to ensure pluripotency. Commercial stem cell antibodies, OCT4 (Abcam), SSEA-1 (Millipore), and NANOG (Abcam), were used for ICC verification. The PCR was performed using the primers of stem cell markers *Oct4*, *Nanog*, *Gdf3*, and *Dnmt3b* to assume pluripotency of the purified GFP positive stem cell population¹⁸.

Embryoid body formation

mGriPSC colonies were manually picked based on morphology and treated with 0.05% Trypsin-EDTA (GIBCO) for 2-3 minutes to dissociate the colonies. The cells were then transferred to plates coated with 2% poly-HEMA in ethanol and cultured in suspension in EB media, consisting of DMEM-F12, 15% knock-out serum replacement (KOSR), 15% HI FBS, 1 mM L-glutamine, 0.1 mM 2-mercaptoethanol, 1% non-essential amino acids (NEAA; Invitrogen, Grand Island, New York), and 1% antibiotic-antimycotic solution (Invitrogen). Cells were cultured in suspension for 20 days, changing the media to fresh EB media every three days, without disturbing the EBs. After 20 days in suspension, EBs were transferred and attached to gelatin-coated plates for future analysis.

Fluorescence-activated cell sorting

To further purify the subpopulation of presumptive ovarian and oocyte cells from the differentiated mGriPSCs-GFP cells, FACS was employed, using the ovarian surface receptor, AMHR2. To prepare for FACS, EBs were dissociated with 0.05% trypsin EDTA to generate a single cell suspension and passed through a 40-µm filter. The cells were then stained with AMHR2 primary antibody for one hour, rinsed, and then treated with anti-mouse Alexa Fluor 488 secondary antibody (Life Technologies/Invitrogen). Using BD FACSAria multicolor high-speed sorter and FACSDiva version 6.1.2 software (BD Biosciences, Franklin Lakes, New Jersey), cells were separated into either AMHR2+ and AMHR2- groups. AMHR2+ and AMHR2- sorted cells were subsequently plated onto gelatin-coated plates and cultured in EB media for one week.

FACS was additionally utilized for cell count analysis for cells positively expressing oocyte and ovarian markers ZP1 and GJA1 in cultures containing different concentrations of HFF. mGriPSCs were cultured in EB media containing different concentrations of HFF to determine if HFF could influence the differentiation of mGriPSCs into presumptive ovarian or oocyte cells. The difference in the percentage of ZP1 and GJA1 expression from media containing 0%, 1%, and 5% HFF by volume was calculated by FACS cell count analysis at day 9 and day 15.

FACS cell count analysis was also used to measure the expression of oocyte markers BOULE, DDX4, GDF9, and ZP2 at day 15 in each of the top layer cells from the 6 different co-culture conditions (Supp Fig. S7 and S8).

Human Follicular Fluid (HFF) acquisition

The following protocol involving human participants has been approved by Partners Human Research Committee (PHRC), the Institutional Review Board (IRB) of Partners HealthCare, protocol #2011P000795. All experiments were performed in accordance with relevant

guidelines and regulations. We confirm that written informed consent was obtained from all participants. HFF was obtained from our institution's In Vitro Fertilization (IVF) laboratory as discarded tissue from consenting patients. Oocyte retrievals were performed as part of the patients' routine care. After transvaginal ultrasound-guided aspiration of oocytes as well as the follicular fluid was completed, discarded HFF was collected as part of the approved IRB protocol, anonymized, pooled from different patients into one collection tube, and transferred to the research laboratory. Freshly obtained HFF were centrifuged at 1500 RPM for 5 min to create a pellet of cumulus granulosa cells, excessive red blood cells, and all suspended biomaterials. The supernatant was collected and passed through a 0.22µm filter to remove impurities and contaminants. A standard endocrine assay was used to determine concentration of E2, FSH, and LH in HFF samples. Filtered HFF were frozen at -80°C until necessary cell culture use.

***In vitro* and *in vivo* ovarian function restoration experiments**

***In vitro*: Co-culture experiment**

mGriPSCs were collected from various stages of their maturation, as was previously described above. No cells, irradiated MEFs, mouse G4 ESCs, unsorted mGriPSC-GFP EBs, or AMHR2+ mGriPSCs-GFP were plated as bottom layers on a trans-well, while mGriPSC stem cells, suspended mGriPSCs-EBs, or attached mGriPSCs-EBs were cultured on top of the trans-wells. The different bottom and top layer cell types therefore created different co-culture conditions. Cell cultures were grown for 15 days, collecting media every 3 days and replacing the volume of the collected media with fresh culture media (Supp Fig S3). This media was used for ELISAs to measure AMH and E2 concentrations at each timepoint (day 0, 3, 6, 9, 12, and 15). At day 15, the bottom layer of cells that were cultured beneath mGriPSCs were used for RNA extraction for RT-PCR. All top layer cell types were analyzed by measuring relative gene expression of *Zp1*, *Ddx4*, *Boule*, and *Blimp* using RT-qPCR. Further, cells positively expressing BOULE, DDX4, GDF9, and ZP2 was isolated from this top layer of cells via FACS (Supp Fig S7 and S8). Lastly, top layer cells were stained for DDX4 and ZP1 for immunocytochemistry analysis. Detailed experimental protocols are described below under the section titled "Analysis of mGriPSC and mGriPSC-GFP differentiation."

***In vivo*: Ovarian function restoration in chemotherapy treated nude mice**

Mouse gonadotoxic treatment and intramuscular cell injection

Female B6.Cg-Foxn1^{nu/nu} mice were received from Jackson Labs (Bar Harbor, ME). Mice were randomized into four groups 1) Control, 2) Chemotherapy with no stem cell injection, 3) Chemotherapy with unsorted mGriPSCs injection, and 4) Chemotherapy with sorted mGriPSCs injections. The control group contained four mice, while all other groups had three. Twelve days after arrival, six-week old mice were superovulated with 5 IU of pregnant mare serum gonadotropin followed 48-hours later by 5 IU of human chorionic gonadotropin to synchronize the mice's menstrual cycles. Three weeks later, premature ovarian insufficiency was induced by single intraperitoneal injections of busulfan (12 mg/kg) and cyclophosphamide (120 mg/kg). Control mice received 100 µl of vehicle (10% DMSO in PBS). After an additional three weeks, experimental mice received intramuscular injections of 2 million unsorted mGriPSCs, sorted mGriPSCs, or vehicle into the left thigh. Hormone synthesis was analyzed and compared between mice that received chemotherapy and controls. Teratomas were measured in mice that received unsorted injections, while no teratomas were detected in mice that received sorted injections.

Mouse gonadotoxic treatment and intraovarian cell injection

Mice were randomized into the same four groups as described above, but this time there were five mice in each group. Chemotherapy was administered in eight-week old nude mice as described above. One week after chemotherapy administration, mice underwent laparotomy with intraovarian injection of either sorted or unsorted mGriPSCs. The laparotomy was performed by placing the mice under isoflurane anesthesia, then infiltrating the ventral midline with a 1:1 mixture of lidocaine and bupivacaine. A midline anterior vertical laparotomy was made under sterile technique. In each case, the left ovary was gently elevated and injected with 2 million cells suspended in PBS using a 27-gauge needle. The ovary was then returned to the abdomen and the abdominal wall closed in two layers using suture. Mice receive 72 hours of meloxicam for post-operative analgesia. Experiments were repeated twice.

Oocyte retrieval

After the mice were sacrificed, their oviducts were obtained using standard techniques. The oviducts were punctured with a 28-gauge needle and washed with 1 ml of PBS with calcium and magnesium to release the cumulus-oocyte complexes from the ampullary regions. To release the cumulus cells from surrounding the oocytes, the cumulus-oocyte complexes were treated with potassium simplex optimized medium (KSOM) with penicillin-streptomycin containing 200 IU/ml hyaluronidase at 37°C for 3 minutes and then washed three times using fresh KSOM. Oocytes were cultured in KSOM at 37°C and 5% CO₂.

Oocyte activation

Oocytes were activated via calcium ionophore activation or sperm fertilization. Oocytes that were activated by a calcium ionophore had hyaluronic acid stripped oocytes treated with KSOM and A23187 Calcium Ionophore overnight at 37°C in 5% CO₂. Using a phase-contrast light microscope (Zeiss, Oberkochen, Germany), oocytes, cultured in KSOM at 37°C in 5% CO₂, were observed for 3 days for any signs of activation. Oocytes that were not activated by a calcium ionophore were treated with sperm extracted from the testes of C57BL6/J mice and observed for any signs of fertilization. To store for future RNA extraction procedures, oocytes, granulosa cells, and half of each ovary were snap frozen in liquid nitrogen. The other half of the ovary was submerged in optimal cutting temperature (OCT) compound (ThermoFisher, Houston, TX), placed on dry ice to freeze, and stored in -80°C freezer for future IHC analysis.

Processing of control ovarian tissues

Untreated C57BL6/J mice were sacrificed, and their ovaries were excised, fixed in cold 4% paraformaldehyde/4% sucrose, and processed for paraffin embedding. Serial sectioned slides of the ovaries were stained by hematoxylin and eosin (H&E) as well as immunostained for oocyte and ovarian markers listed above. The serial sectioning of control ovaries was necessary to provide a comparative staining for our experimental cells and tissues, displaying ovarian and oocyte markers.

Analysis of mGriPSCs and mGriPSCs-GFP differentiation

Ovarian and oocyte markers were used to qualitatively characterize the differentiation of mGriPSCs into presumptive ovarian and oocyte cells.

RT-PCR analysis

RT-PCRs were performed on mGriPSCs as well as the mGriPSCs-GFP to ensure that the differentiation of the cells was not influenced by the insertion of GFP (Supp Fig S1A). The

mGriPSCs-GFP were further analyzed by performing RT-PCRs for both the cells before FACS and after FACS (AMHR2+ cells). RT-PCRs were also performed for the bottom layer of co-culture cells described below using ovarian markers *Cyp19a1*, inhibin β -A (*Inhb*), forkhead box protein L2 (*Foxl2*), *Fshr*, *Gja1*, and *Amh*. After RNA was extracted using commercially available kits (Qiagen, Germantown, MD), reverse transcribed cDNA was synthesized via a qScript cDNA Synthesis kit (Quanta Biosciences, Gaithersburg, MD). The cDNA along with DNA polymerase (Promega, Madison, WI) were combined with corresponding primers for ovarian markers (anti-Müllerian hormone receptor (*Amhr2*), aromatase (*Cyp19a1*), follicle-stimulating hormone receptor (*Fshr*), gap junction alpha-1 (*Gja1*), and anti-Müllerian hormone (*Amh*)) and oocyte markers (DEAD-box helicase 4 (*Ddx4*), Boule, and PR domain zinc finger protein-1 (*Blimp-1*)), with β -actin as a positive control to analyze the differentiation of mGriPSCs. Cycling conditions were 95°C for 3 minutes, 35 repetitions of (95 °C for 1 minute, 58.5 °C for 1 minute, and 72 for 1 minute) and 72 °C for 10 minutes in a thermocycler (Bio-Rad). Amplified products were separated on 1.0% agarose gel electrophoresis (Thermofisher) to qualitatively analyze the expression of tested biomarkers.

RT-qPCR analysis from tissues

Freshly harvested tissue from 3 sacrificed mice in each condition were snap-frozen in liquid nitrogen for 30 seconds and stored in -80 °C overnight. Frozen samples were thawed and ground with mortar and pestle and then homogenized with lysis buffer. These homogenized and lysed tissue samples were then processed for RNA extraction as described above. After cDNA synthesis, 2 ng of cDNA was used in each qPCR reaction well. Primers for the oocyte markers listed above with the addition of oocyte marker Zona Pellucida-1 (*Zp1*) were used for qPCR analysis of co-cultured cells, while *Zp1*, *Boule*, *Ddx4*, *Gja1*, *Inhb*, *Cyp19a1*, and *Amh* were used for primers for qPCR of ovary tissues. Each set of primers as well as Power SYBR Green reaction mix (Applied Biosystems, Foster City, CA) were used for qPCR reactions. A QuantStudio 3 (Applied Biosystems) real-time thermocycler was used with the cycling conditions of 50 °C for 2 minutes, 95 °C for 10 minutes, and 60 repetitions of (95 °C for 1 minute and 60 °C for 2.5 minutes). Fold changes in gene expression were measured using the $2^{-\Delta\Delta}$ Ct technique with β -actin as the endogenous control gene for relative quantification. qPCRs for the ovarian tissue used ovaries that were not treated with chemotherapy nor injected with stem cells as the referent control against which fold change in gene expression was compared in the treated ovaries. mGriPSCs-GFP in one of three developmental stages (1. Stem cells, 2. Suspended EBs, or 3. Attached EBs) were co-cultured on the top layer of a transwell with either sorted AMHR2+ mGriPSCs-GFP or unsorted, differentiated mGriPSCs-GFP on the bottom layer. qPCR was used to quantify relative gene expression of oocyte markers in the top layer of cells, comparing the effect of co-culturing with sorted cells versus unsorted cells on the bottom layer. When analyzing relative gene expression via the $2^{-\Delta\Delta}$ Ct technique, cells from each developmental stage were compared only with cells from the same developmental stage, thus focusing the analysis on the effect of co-culturing with sorted cells versus unsorted cells.

Immunocytochemistry/Immunohistochemistry (ICC/IHC)

Pre-warmed 0.05% Trypsin-EDTA was used to dissociate mGriPSC EBs so that they could be subsequently reattached to gelatin-coated plates as a more ideal visual monolayer of cells. Cells or prepared histological tissue samples were fixed in cold 4% paraformaldehyde (4°C)/4% sucrose for 30 minutes at room temperature and rinsed three times with 1x phosphate-buffered saline (PBS; Corning, Corning, NY) for 5 minutes. The cells were blocked with 2% donkey serum,

iPSC -based restoration of ovarian function following gonadotoxic chemotherapy

10 mg/mL bovine serum albumin, and 1% Triton-X for 30 minutes. The primary antibodies for ovarian markers, AMHR2, CYP19a1, FOXL2, FSHR (Santa Cruz, Dallas, TX), INHB (Santa Cruz), GJA1, and primary antibodies for oocyte markers, Deleted in zoospermia-like (DAZL), DEAD-Box Helicase 4 (DDX4), zona pellucida glycoprotein 1 (ZP1; Santa Cruz), and zona pellucida glycoprotein 2 (ZP2; Santa Cruz), were then applied for 2 hours at room temperature, followed by three 5 min PBS rinses before the secondary antibodies (Thermofisher) were applied for 1 hour in a dark environment at room temperature. After the secondary antibody incubation, the cell and tissue samples were rinsed 3 times for 5 minutes with PBS, followed by the application of 4',6-diamidino-2-phenylindole (DAPI) for 10 minutes to visualize the nuclei. Finally, the samples were rinsed three last times with PBS for 5 minutes before performing fluorescent microscopy using a Zeiss Axiovert (Zeiss Microscopes) 40 CFL and ImagerM2.

ELISA and hormone analysis

Estradiol concentrations within attached EB media were analyzed using commercially available enzyme-linked immunosorbent assay (ELISA) kits (Abnova, Zhongli, Taiwan). Three media samples from each condition were collected at day 0, 6, 9, 12, and 15. Additionally, estradiol concentrations from media containing 0%, 0.5%, 1%, 2%, 3%, and 5% HFF were measured at day 0, 9, and 15 using ELISA kits. Estradiol, progesterone, and Anti Mullerian hormone (AMH) concentrations were also analyzed via ELISA kits for either the mGriPSC-GFP pre-FACS and post-FACS cell analysis at days 0, 3, 6, 9, 12, and 15, or for the 6 different *in vitro* co-culture conditions at days 0, 3, 6, 9, 12, and 15, or from blood serum from the four different mouse injection groups at three timepoints (baseline, pre-chemo, and pre-sacrifice) from the *in vivo* mouse injections.

Data availability

The full data supporting this article are available from the corresponding author upon reasonable request.

References

1. Hyman, J. H. & Tulandi, T. Fertility preservation options after gonadotoxic chemotherapy. *Clin. Med. Insights Reprod. Health* **7**, 61–69 (2013).
2. Blumenfeld, Z. Gynaecologic concerns for young women exposed to gonadotoxic chemotherapy. *Curr. Opin. Obstet. Gynecol.* **15**, 359–370 (2003).
3. Srikanthan, A. *et al.* Fertility preservation in post-pubescent female cancer patients: A practical guideline for clinicians. *Mol. Clin. Oncol.* **8**, 153–158 (2018).
4. Bastings, L., Baysal, Ö., Beerendonk, C. C. M., Braat, D. D. M. & Nelen, W. L. D. M. Referral for fertility preservation counselling in female cancer patients. *Hum. Reprod.* **29**, 2228–2237 (2014).
5. Luke, B. *et al.* Assisted reproductive technology use and outcomes among women with a history of cancer. *Hum. Reprod.* **31**, 183–189 (2016).
6. Anderson, R. A. *et al.* The impact of cancer on subsequent chance of pregnancy: a population-based analysis. *Hum. Reprod. Oxf. Engl.* **33**, 1281–1290 (2018).
7. Sklavos, M. M., Giri, N., Stratton, P., Alter, B. P. & Pinto, L. A. Anti-Müllerian Hormone Deficiency in Females With Fanconi Anemia. *J. Clin. Endocrinol. Metab.* **99**, 1608–1614 (2014).
8. Daum, H., Peretz, T. & Laufer, N. BRCA mutations and reproduction. *Fertil. Steril.* **109**, 33–38 (2018).
9. Rose, S. R. *et al.* Late endocrine effects of childhood cancer. *Nat. Rev. Endocrinol.* **12**, 319 (2016).
10. Stava, C. J., Jimenez, C., Hu, M. I. & Vassilopoulou-Sellin, R. Skeletal sequelae of cancer and cancer treatment. *J. Cancer Surviv.* **3**, 75–88 (2009).

11. Podfigurna-Stopa, A. *et al.* Premature ovarian insufficiency: the context of long-term effects. *J. Endocrinol. Invest.* **39**, 983–990 (2016).
12. Lindau, S. T., Abramsohn, E. M. & Matthews, A. C. A manifesto on the preservation of sexual function in women and girls with cancer. *Am. J. Obstet. Gynecol.* **213**, 166–174 (2015).
13. Boyne, D. J. *et al.* Long-term risk of cardiovascular mortality in lymphoma survivors: A systematic review and meta-analysis. *Cancer Med.* **7**, 4801–4813 (2018).
14. Fish, J. D. Part 1: Hormone Replacement for Survivors of Childhood Cancer with Ovarian Failure—When Is It Worth the Risk? *J. Pediatr. Adolesc. Gynecol.* **24**, 98–101 (2011).
15. Sullivan, S. D., Sarrel, P. M. & Nelson, L. M. Hormone replacement therapy in young women with primary ovarian insufficiency and early menopause. *Fertil. Steril.* **106**, 1588–1599 (2016).
16. Shanis, D. *et al.* Female long-term survivors after allogeneic hematopoietic stem cell transplantation: evaluation and management. *Semin. Hematol.* **49**, 83–93 (2012).
17. Woodard, T. L. & Bolcun-Filas, E. Prolonging Reproductive Life after Cancer: The Need for Fertoprotective Therapies. *Trends Cancer* **2**, 222–233 (2016).
18. Anchan, R. *et al.* Efficient Differentiation of Steroidogenic and Germ-Like Cells from Epigenetically-Related iPSCs Derived from Ovarian Granulosa Cells. *PLOS ONE* **10**, e0119275 (2015).
19. Guven, S. *et al.* Functional Maintenance of Differentiated Embryoid Bodies in Microfluidic Systems: A Platform for Personalized Medicine. *STEM CELLS Transl. Med.* **4**, 261–268 (2015).

20. Lipskind, S. *et al.* An Embryonic and Induced Pluripotent Stem Cell Model for Ovarian Granulosa Cell Development and Steroidogenesis. *Reprod. Sci.* **25**, 712–726 (2017).
21. Choi, J. K. *et al.* Bio-inspired solute enables preservation of human oocytes using minimum volume vitrification. *J. Tissue Eng. Regen. Med.* **12**, e142–e149 (2018).
22. Su, Y.-Q., Sugiyura, K. & Eppig, J. J. Mouse oocyte control of granulosa cell development and function: paracrine regulation of cumulus cell metabolism. *Semin. Reprod. Med.* **27**, 32–42 (2009).
23. Hortobagyi, G., Buzdar, A. U., Marcus, C. & Smith, T. Immediate and long-term toxicity of adjuvant chemotherapy regimens containing doxorubicin in trials at MD Anderson Hospital and Tumor Institute. *NCI Monogr. Publ. Natl. Cancer Inst.* 105–109 (1986).
24. Rebar, R. W., Morandini, I. C., Erickson, G. F. & Petze, J. E. The Hormonal Basis of Reproductive Defects in Athymic Mice: Diminished Gonadotropin Concentrations in Prepubertal Females. *Endocrinology* **108**, 120–126 (1981).
25. Jiang, Y. *et al.* Accelerated ovarian aging in mice by treatment of busulfan and cyclophosphamide. *J. Zhejiang Univ. Sci. B* **14**, 318–324 (2013).
26. Anchan, R. M., Salas, S., Ng, N. & Gerami-Naini, B. Induced Pluripotent Stem Cells from Ovarian Tissue. *Curr. Protoc. Hum. Genet.* (2017).
27. Gerami-Naini, B. *et al.* Trophoblast Differentiation in Embryoid Bodies Derived from Human Embryonic Stem Cells. *Endocrinology* **145**, 1517–1524 (2004).
28. Geijsen, N. *et al.* Derivation of embryonic germ cells and male gametes from embryonic stem cells. *Nature* **427**, 148 (2003).

29. Tilly, J. L. *et al.* Embryonic Stem Cell–Derived Granulosa Cells Participate in Ovarian Follicle Formation In Vitro and In Vivo. *Reprod. Sci.* **20**, 524–535 (2013).
30. Woodruff, T. K. *et al.* In vitro grown human ovarian follicles from cancer patients support oocyte growth. *Hum. Reprod.* **24**, 2531–2540 (2009).
31. Hayashi, K., Hikabe, O., Obata, Y. & Hirao, Y. Reconstitution of mouse oogenesis in a dish from pluripotent stem cells. *Nat. Protoc.* **12**, 1733 (2017).
32. Yamashiro, C. *et al.* Generation of human oogonia from induced pluripotent stem cells in vitro. *Science* (2018). doi:10.1126/science.aat1674
33. Fu, X., He, Y., Xie, C. & Liu, W. Bone marrow mesenchymal stem cell transplantation improves ovarian function and structure in rats with chemotherapy-induced ovarian damage. *Cytotherapy* **10**, 353–363 (2008).
34. Christianson, M. S. & Segars, J. Unleashing the potential of stem cells to help poor responders. *Fertil. Steril.* **110**, 410–411 (2018).
35. Liu, J. *et al.* Homing and Restorative Effects of Bone Marrow-Derived Mesenchymal Stem Cells on Cisplatin Injured Ovaries in Rats. *Mol. Cells* **37**, 865–872 (2014).
36. Hayes, E. *et al.* Intra-cellular mechanism of Anti-Müllerian hormone (AMH) in regulation of follicular development. *Mol. Cell. Endocrinol.* **433**, 56–65 (2016).
37. Kushnir, V. A., Seifer, D. B., Barad, D. H., Sen, A. & Gleicher, N. Potential therapeutic applications of human anti-Müllerian hormone (AMH) analogues in reproductive medicine. *J. Assist. Reprod. Genet.* **34**, 1105–1113 (2017).
38. Broer, S. L., Broekmans, F. J. M., Laven, J. S. E. & Fauser, B. C. J. M. Anti-Müllerian hormone: ovarian reserve testing and its potential clinical implications. *Hum. Reprod. Update* **20**, 688–701 (2014).

39. Fleming, R., Seifer, D. B., Frattarelli, J. L. & Ruman, J. Assessing ovarian response: antral follicle count versus anti-Müllerian hormone. *Reprod. Biomed. Online* **31**, 486–496 (2015).
40. Johnson, L. N. C. *et al.* Antimüllerian hormone and antral follicle count are lower in female cancer survivors and healthy women taking hormonal contraception. *Fertil. Steril.* **102**, 774-781.e3 (2014).
41. Chan, J. L., Johnson, L. N. C., Efymow, B. L., Sammel, M. D. & Gracia, C. R. Outcomes of ovarian stimulation after treatment with chemotherapy. *J. Assist. Reprod. Genet.* **32**, 1537–1545 (2015).
42. Tal, R., Tal, O., Seifer, B. J. & Seifer, D. B. Antimüllerian hormone as predictor of implantation and clinical pregnancy after assisted conception: a systematic review and meta-analysis. *Fertil. Steril.* **103**, 119-130.e3 (2015).
43. Dunlop, C. E. & Anderson, R. A. Uses of anti-Müllerian hormone (AMH) measurement before and after cancer treatment in women. *Maturitas* **80**, 245–250 (2015).
44. Santoro, N. Mechanisms of premature ovarian failure. *Ann. Endocrinol.* **64**, 87–92 (2003).
45. Kitamura, T. *et al.* Retrovirus-mediated gene transfer and expression cloning: powerful tools in functional genomics. *Exp. Hematol.* **31**, 1007–1014 (2003).

Acknowledgements

Center for Infertility and Reproductive Surgery (CIRS) Research Development Award (CRDA), Division of Reproductive Endocrinology and Infertility, and the Department of Obstetrics, Gynecology, and Reproductive Biology, Brigham and Women's Hospital, Harvard Medical School.

The authors would also like to thank Ms. Cecelia Chan of The Siezen Foundation for research funding support, Dr. Robert Barbieri for editorial comments, Maya Seshan for editorial assistance, and Mazhar Chaudhry for assistance with endocrine analyses.

Author contributions

K.E. and R.M.A. developed the research design. E.R.D., E.S.G., K.E., and R.M.A. wrote the manuscript. A.G., A.M., E.R.D., K.E., K.U.D., N.W.N., N.D., and R.M.A. performed the experiments and collected data. A.M., K.U.D., N.W.N., and R.M.A. analyzed the data.

Competing interest statement

The authors declare no competing interests.

Corresponding author

Correspondence to Raymond M. Anchan, MD. PhD.